

# The finite source size effect and the wave optics in gravitational lensing

Norihito Matsunaga and Kazuhiro Yamamoto

Graduate School of Sciences, Hiroshima University, Higashi-hiroshima, 739-8526, Japan

**Abstract.** We investigate the finite source size effect in the context of the wave optics in the gravitational lensing. The magnification of an extended source is presented in an analytic manner for the singular isothermal sphere lens model as well as the point mass lens model with the use of the thin lens approximation. The condition that the finite source size effect becomes substantial is demonstrated. As an application, we discuss possible observational consequences of the finite source size effect on astrophysical systems.

## 1. Introduction

Gravitational lensing is a characteristic phenomenon of the general relativity and has become a very important tool in the fields of cosmology and astrophysics [1, 2]. For example, the existence of the massive compact halo objects (MACHO) in the Galaxy was revealed by the detection of the lensed amplification of stellar objects [3], and the recent measurements of the cosmic shear field provide a constraint on the matter distribution independently of the clustering bias [4, 5, 6, 7]. Promisingly the gravitational lensing will play a more important role with progress in the capability of observational facilities in future. For example, it will be a useful probe of the nature of the dark energy [8, 9, 10, 11].

As a fundamental aspect of the gravitational lensing, the effect of wave optics has been investigated by many authors [12, 13, 14, 1]. Very recently, this subject is revisited by several authors, motivated by a possible phenomenon which might be observed in the future gravitational wave experiments [15, 16, 17, 18, 19, 20, 21, 22, 23, 24, 25, 26, 27]. In the context of the wave optics of gravitational lensing, the argument on the distance-redshift relation is also revisited [28].

The present paper focuses on the finite source size effect in the wave optics of the gravitational lensing. In the first half part of this paper, we present an analytic solution for the wave equation with the singular isothermal sphere lens model. In general, it is difficult to obtain an exact solution for general lens model, excepting a few simple lens models [29, 26]. Therefore it is useful to obtain such analytic solution for the wave equation. The wave optics of the singular isothermal sphere lens has been investigated by

Takahashi and Nakamura using a numerical technique [30, 31]. We present the analytic expression for the amplification factor, which is the first aim of the present paper. Then, as an application of the analytic formula, we investigate the finite source size effect in the wave optics, which is the other aim of the present paper. Using the analytic formula, we consider the energy spectrum from an extended source with a Gaussian distribution of surface brightness [32]. We investigate the condition that the finite source size effect becomes important in the wave optics, including the case near the caustic in the limit of the geometrical optics.

This paper is organized as follows: In section 2, we review the basic formulas for the wave optics in gravitational lensing. The limit of the geometrical optics is also reviewed for self-containment. Then, we present analytic expressions of the amplification factor for the point mass lens model as well as the singular isothermal sphere lens model in section 3. In section 4, we investigate the finite source size effect with the use of the analytic formulas. In section 5, the validity of the approximation of the point source is discussed for the gravitational wave from a compact binary. The femtolensing of the gamma ray burst source is also revisited [32, 33], and the finite source size effect is considered. The last section is devoted to summary and conclusions. Throughout this paper, we use the unit in which the light velocity equals 1.

## 2. Review of Basic Formalism

### 2.1. Wave Optics under the Thin Lens Approximation

We consider the background spacetime with the line element,

$$ds^2 = g_{\mu\nu}dx^\mu dx^\nu = -(1 + 2U(\vec{r}))dt^2 + (1 - 2U(\vec{r}))d\vec{r}^2, \quad (1)$$

where  $U(\vec{r})$  is the Newtonian gravitational potential with the condition  $U(\vec{r}) \ll 1$ . On the Newtonian background spacetime, we consider the wave propagation of the scalar field  $\Phi$ . The propagation of the electro-magnetic wave and the gravitational wave can be well described by the scalar wave equation [12, 1], which is given by

$$\partial_\mu(\sqrt{-g}g^{\mu\nu}\partial_\nu\Phi) = 0. \quad (2)$$

This is rewritten as

$$(\nabla^2 + \omega^2)\Phi = 4\omega^2U(\vec{r})\Phi, \quad (3)$$

on the spacetime with the line element (1), where we assume the monochromatic wave with the angular frequency  $\omega$ . In the present paper we consider the spherically symmetric potential.

It is useful to introduce the amplification factor  $F$  (which is called the transmission factor in Ref. [1]) by  $F = \Phi/\Phi_0$ , where  $\Phi_0$  is the wave amplitude in the absence of the gravitational potential,  $U = 0$ . Then, under the thin lens approximation, the amplification factor is given by

$$F(\omega, \vec{\eta}) = \frac{d_S}{d_L d_{LS}} \frac{\omega}{2\pi i} \int_{-\infty}^{\infty} d^2\xi \exp[i\omega\hat{\phi}(\vec{\xi}, \vec{\eta})], \quad (4)$$

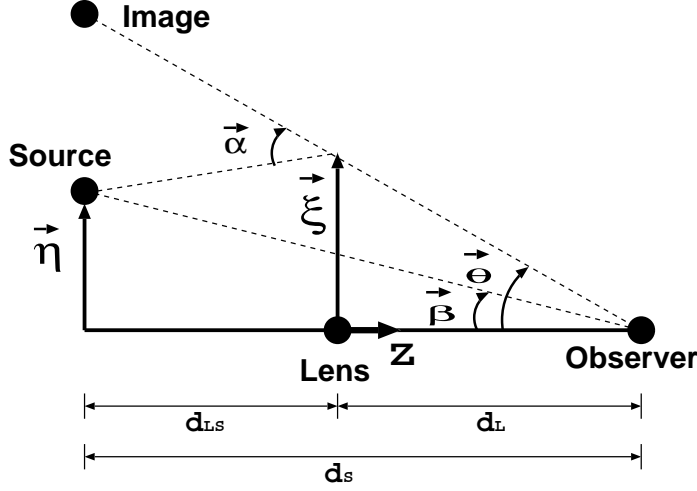


**Figure 1.** Configuration of the source, the lens and the observer.  $d_L$ ,  $d_S$  and  $d_{LS}$  are the distances between the lens and the observer, the source and observer, and the lens and the source, respectively.  $\vec{\eta}$  is the position of the (point) source, and  $\vec{\xi}$  is the impact parameter.  $\vec{\beta}$  is the unlensed source position angle,  $\vec{\theta}$  is the position angle of the image, and the deflection angle is  $\vec{\alpha}$ . This sketch is based on the thin lens approximation that the wave is scattered only on the thin lens plane.

where  $\hat{\phi}(\vec{\xi}, \vec{\eta})$  is the time delay function (Fermat's potential), which is given by

$$\hat{\phi}(\vec{\xi}, \vec{\eta}) = \frac{d_L d_S}{2d_{LS}} \left( \frac{\vec{\xi}}{d_L} - \frac{\vec{\eta}}{d_S} \right)^2 - \hat{\psi}(\vec{\xi}), \quad (5)$$

where  $d_L$  is the distance between the lens and the source,  $d_S$  is the distance between the source and the observer,  $d_{LS}$  is the distance between the lens and the source, respectively, (see Figure 1 for the configuration of the lensing system and the definition of variables). In general, we may add a term  $\hat{\phi}_m(\vec{\eta})$  in the right hand side of (5) [30]. However, the inclusion does not alter our arguments and we omit it. The two dimensional gravitational deflection potential is defined by

$$\hat{\psi}(\vec{\xi}) = 2 \int_{-\infty}^{\infty} dz U(\vec{\xi}, z). \quad (6)$$

Note that  $|F| = 1$  in the absence of the lens potential  $U = 0$ .

The above formulas can be generalized so as to take the cosmological expansion into account. Assuming that the wavelength of the scalar waves is much shorter than the horizon scale, Eq. (4) is generalized as

$$F(\omega, \vec{\eta}) = \frac{d_S}{d_L d_{LS}} \frac{\omega(1+z_L)}{2\pi i} \int_{-\infty}^{\infty} d^2\xi \exp[i\omega(1+z_L)\hat{\phi}(\vec{\xi}, \vec{\eta})], \quad (7)$$

where  $d_L$ ,  $d_S$ , and  $d_{LS}$  are the angular diameter distances, and  $z_L$  is the redshift of the lens object.

It is useful to rewrite the amplification factor  $F$  in terms of dimensionless quantities. We introduce

$$\vec{x} = \frac{\vec{\xi}}{\xi_0}, \quad \vec{y} = \frac{d_L}{\xi_0 d_S} \vec{\eta}, \quad (8)$$

$$w = \frac{d_S}{d_L d_{LS}} \xi_0^2 (1 + z_L) \omega, \quad (9)$$

$$\psi = \frac{d_L d_{LS}}{d_S \xi_0^2} \hat{\psi}, \quad (10)$$

where  $\xi_0$  is the normalization constant of the length in the lens plane, for which we adopt

$$\xi_0 = \theta_E d_L, \quad (11)$$

where  $\theta_E$  is the Einstein angle, i.e., the solution of the lens equation (16) with  $\vec{\beta} = 0$ . (see below.) The effect of the wave optics is characterized by the dimensionless parameter  $w$ . We also introduce the dimensionless time delay function by

$$T(\vec{x}, \vec{y}) = \frac{d_L d_{LS}}{d_S \xi_0^2} \hat{\phi}(\vec{\xi}, \vec{\eta}) = \frac{1}{2} |\vec{x} - \vec{y}|^2 - \psi(\vec{x}). \quad (12)$$

Then, the amplification factor is written as

$$F(w, \vec{y}) = \frac{w}{2\pi i} \int_{-\infty}^{\infty} d^2x \exp[iwT(\vec{x}, \vec{y})]. \quad (13)$$

In the case of the spherically symmetric lens model, the gravitational deflection potential  $\psi(\vec{x})$  depends only on  $x = |\vec{x}|$ . Then, the amplification factor is reduced to the relatively simple formula

$$F(w, y) = -iw e^{\frac{i}{2}wy^2} \int_0^{\infty} dx x J_0(wxy) \exp\left[iw\left(\frac{1}{2}x^2 - \psi(x)\right)\right], \quad (14)$$

where  $J_0(z)$  is the Bessel function of the zeroth order and  $y = |\vec{y}|$ .

## 2.2. Geometrical Optics Approximation

In this subsection we consider the limit of the short wave length in the wave optics ( $w \gg 1$ ), which reproduces the conventional geometrical optics in the gravitational lensing. In the limit of the geometrical optics, the diffraction integral (13) is evaluated around the stationary points of the time delay function  $T(\vec{x}, \vec{y})$ . Thus the stationary points are determined by the solution of  $\nabla_x T(\vec{x}, \vec{y}) = 0$ , which is written as

$$\vec{y} = \vec{x} - \nabla_x \psi(\vec{x}). \quad (15)$$

This is the lens equation to determine the image position  $\vec{x}_j$ . Eq. (15) is rewritten as

$$\vec{\beta} = \vec{\theta} - \vec{\alpha}(\vec{\theta}), \quad (16)$$

where  $\vec{\beta} = (\xi_0/d_L)\vec{y}$  is the angular position of the source,  $\vec{\theta} = (\xi_0/d_L)\vec{x}$  is the angular position of the images, and  $\vec{\alpha} = (\xi_0/d_L)\nabla_x \psi(\vec{x})$  is the deflection angle (see Figure 1).

The time delay function  $T(\vec{x}, \vec{y})$  is expressed around the  $j$ -th image position  $\vec{x}_j$  as

$$T(\vec{x}, \vec{y}) = T(\vec{x}_j, \vec{y}) + \frac{1}{2} \sum_{a,b=1,2} \partial_a \partial_b T(\vec{x}_j, \vec{y}) X_a X_b + \mathcal{O}(X^3), \quad (17)$$

where  $\vec{X} = \vec{x} - \vec{x}_j$ . Here, the term in proportion to  $\vec{X}$  vanishes because  $\vec{x}_j$  is the stationary point of  $T(\vec{x}, \vec{y})$ . Inserting Eq. (17) into Eq. (13), we obtain the amplification

factor in geometrical optics limit [15, 30, 31]

$$F_{geo}(w, \vec{y}) = \sum_j |\mu(\vec{x}_j)|^{1/2} \exp \left[ iwT(\vec{x}_j, \vec{y}) - i\frac{n_j}{2}\pi \right], \quad (18)$$

where the magnification of the  $j$ -th image is  $\mu(\vec{x}_j) = 1/\det(\partial\vec{y}/\partial\vec{x}_j)$  and  $n_j = 0, 1, 2$  when  $\vec{x}_j$  is a minimum, saddle, maximum point of  $T(\vec{x}, \vec{y})$ , respectively. For the case of multi-lensed images, in the geometrical optics approximation, the expression (18) means that the observed wave is described by a superposition of each wave with the amplitude,  $|\mu(\vec{x}_j)|^{1/2}$ , and the phase,  $wT(\vec{x}_j, \vec{y}) - (n_j\pi)/2$  [15].

### 3. Analytic Expressions for the Amplification Factor

In this section we present analytic expressions for the amplification factor (14) for the point mass lens model and the singular isothermal sphere (SIS) lens model. The expression for the point mass lens model is well known [12, 13, 14, 1]. Recently the amplification factor for the SIS lens model is investigated by Takahashi and Nakamura with the use of a numerical method [30, 31]. However, we derive an analytic expression for the SIS lens model in the present paper. The SIS lens model is often used to study a lensing phenomenon by a galaxy halo and by a cluster of galaxies. In order to understand the wave effect in the lensing by a halo, such an analytic formula is useful. The amplification factor obtained using the analytic expression for the SIS lens model gives us the results consistent with those by Takahashi and Nakamura through their numerical method [30, 31].

#### 3.1. Gravitational Deflection Potential

Let us here summarize the relation between the gravitational deflection potential  $\psi(\vec{x})$  and the density distribution of a lens object (see e.g., [1]). In general the deflection potential is given by

$$\psi(\vec{x}) = 4G \frac{d_L d_{LS}}{d_S} \int_{-\infty}^{\infty} d^2s \Sigma(\vec{s}) \log |\vec{x} - \vec{s}|, \quad (19)$$

where  $\Sigma(\vec{s})$  is surface mass density in lens plane,

$$\Sigma(\vec{x}) = \int_{-\infty}^{\infty} dz \rho(\vec{x}, z), \quad (20)$$

where  $\rho(\vec{x}, z)$  is the mass density distribution of the lens, which is related to the Newtonian potential by  $\nabla^2 U = 4\pi G\rho$ . Thus the lens model is characterized by the mass density distribution  $\rho(\vec{x}, z)$  as well as the gravitational deflection potential  $\psi(\vec{x})$ .

#### 3.2. Point Mass Lens

The gravitational lensing by a black hole and a compact star is described by the point mass lens model, in which we write  $\rho(\vec{x}, z) = M\delta^{(2)}(\vec{\xi})\delta^{(1)}(z)$ , where  $M$  is the mass of

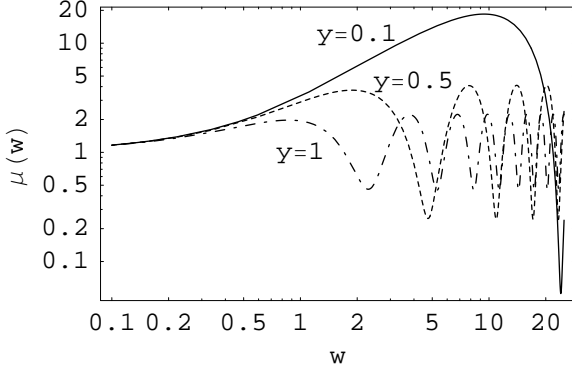


**Figure 2.** Magnification  $\mu(w, y)$  as a function of dimensionless parameter  $w$  for the point mass lens model. Here, the source position is fixed as  $y = 0.1, 0.5, \text{ and } 1$ , respectively.

the lens object. Then, the surface mass density is  $\Sigma(\vec{x}) = M\delta^{(2)}(\vec{\xi}) = M\delta^{(2)}(\xi_0\vec{x})$ . In this model the characteristic Einstein angle  $\theta_E$  is

$$\theta_E = \sqrt{\frac{4GMd_{LS}}{d_L d_S}} \simeq 3 \times 10^{-6} \left(\frac{M}{M_\odot}\right)^{1/2} \left(\frac{d_L d_S / d_{LS}}{1\text{Gpc}}\right)^{-1/2} \text{ arcsec}, \quad (21)$$

and the gravitational deflection potential is given by  $\psi(x) = \log x$ . Using a mathematical integral formula [34], the expression of the amplification factor (14) yields

$$F = e^{\frac{i}{2}w(y^2 + \log(w/2))} e^{\frac{\pi}{4}w} \Gamma\left(1 - \frac{i}{2}w\right) {}_1F_1\left(1 - \frac{i}{2}w, 1; -\frac{i}{2}wy^2\right), \quad (22)$$

where  ${}_1F_1(a, c, z)$  is the confluent hypergeometric function [35]. In this model we have the dimensionless parameter from Eq. (9), which characterizes the wave optics,

$$w = 4GM(1 + z_L)\omega \simeq 1.2 \times 10^{-4}(1 + z_L) \left(\frac{M}{M_\odot}\right) \left(\frac{\nu}{1\text{Hz}}\right). \quad (23)$$

Note that  $w$  has the meaning of the ratio of the Schwarzschild radius to the wavelength of the propagating wave. The wave effect becomes significant when  $w \sim \mathcal{O}(1)$ .

We define the magnification by  $\mu(w, y) \equiv |F(w, y)|^2$ , which gives us the expression

$$\mu(w, y) = \frac{\pi w}{1 - e^{-\pi w}} \left| {}_1F_1\left(\frac{i}{2}w, 1; \frac{i}{2}wy^2\right) \right|^2, \quad (24)$$

from expression (22). The maximum magnification is achieved when  $y = 0$ , which provides the configuration of the Einstein ring,

$$\mu_{max} = \frac{\pi w}{1 - e^{-\pi w}}. \quad (25)$$

Figure 2 shows the magnification (24) as a function of the wave characteristic parameter  $w$  with the source position fixed  $y = 0.1, 0.5, \text{ and } 1$ . For  $w \gtrsim 1$ , the oscillation feature appears due to the interference in the wave effect between the double images (see also Figure 3).

We next consider the approximation based on the geometrical optics explained in the previous section. The point mass lens model has the two images in the geometrical

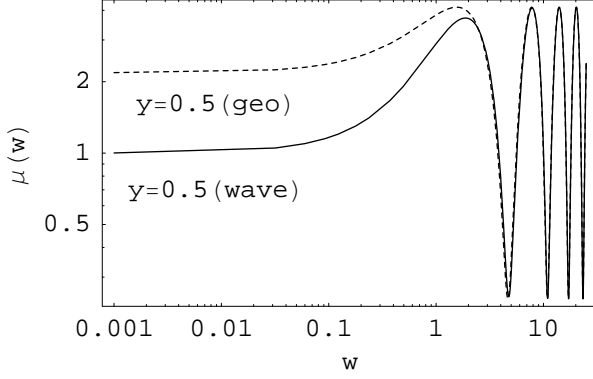


**Figure 3.** Magnification as a function of the dimensionless parameter  $w$ . The solid curve is the result of the wave optics  $\mu(w, y)$ , while the dashed curve is  $\mu_{geo}(w, y)$ . Here, the source position is fixed as  $y = 0.5$ .

optics. Namely, the lens equation has the two solution (the minimum and the saddle points of the time delay function). Then, (18) yields

$$F_{geo}(w, \vec{y}) = |\mu_+|^{1/2} \exp \left[ iw \left( \frac{1}{2} (p_+ - y)^2 - \log |p_+| \right) \right] - i |\mu_-|^{1/2} \exp \left[ iw \left( \frac{1}{2} (p_- - y)^2 - \log |p_-| \right) \right], \quad (26)$$

where the magnification of each image is  $\mu_{\pm} = 1/2 \pm (y^2 + 2)/(2y\sqrt{y^2 + 4})$  and  $p_{\pm} = (1/2)(y \pm \sqrt{y^2 + 4})$ . Then, the corresponding magnification is

$$\mu_{geo}(w, y) = \frac{y^2 + 2}{y\sqrt{y^2 + 4}} + \frac{2}{y\sqrt{y^2 + 4}} \sin \left[ w \left( \frac{1}{2} y \sqrt{y^2 + 4} + \log \left| \frac{\sqrt{y^2 + 4} + y}{\sqrt{y^2 + 4} - y} \right| \right) \right]. \quad (27)$$

Figure 3 shows the magnification (24) and (27), as a function of the parameter  $w$  with the source position fixed  $y = 0.5$ . For  $w \gtrsim 1$ , both the curves agree, and the geometrical optics is a very good approximation. For  $w \lesssim 1$ , however, the two curves are not in good agreement because the geometrical optics approximation is not suitable.

### 3.3. Singular Isothermal Sphere Lens

We next consider the SIS lens model, which can be used for modeling a halo. In this model, the density profile is

$$\rho(\vec{x}, z) = \frac{\sigma_v^2}{2\pi G(|\vec{\xi}|^2 + z^2)} = \frac{\sigma_v^2}{2\pi G(|\xi_0 \vec{x}|^2 + z^2)}, \quad (28)$$

where  $\sigma_v$  is the velocity dispersion. Then, the surface density is given by

$$\Sigma(\vec{x}) = \frac{\sigma_v^2}{2G|\vec{\xi}|} = \frac{\sigma_v^2}{2G\xi_0 x}, \quad (29)$$

and the gravitational deflection potential is given by  $\psi(x) = x$ . The Einstein angle of the SIS lens model is

$$\theta_E = 4\pi\sigma_v^2 \frac{d_{LS}}{d_S} \simeq 3 \times 10^{-5} \left( \frac{\sigma_v}{1\text{km/s}} \right)^2 \left( \frac{d_{LS}}{d_S} \right) \text{ arcsec}, \quad (30)$$

therefore, the dimensionless parameter  $w$  is given by

$$\begin{aligned} w &= (1 + z_L)\omega(4\pi\sigma_v^2)^2 \frac{d_L d_{LS}}{d_S} \\ &\simeq 3 \times (1 + z_L) \left( \frac{\sigma_v}{1\text{m/s}} \right)^4 \left( \frac{\hbar\omega}{1\text{keV}} \right) \left( \frac{d_L d_{LS}/d_S}{1\text{Mpc}} \right) \\ &\simeq 0.01(1 + z_L) \left( \frac{\sigma_v}{1\text{km/s}} \right)^4 \left( \frac{\nu}{1\text{Hz}} \right) \left( \frac{d_L d_{LS}/d_S}{1\text{Gpc}} \right). \end{aligned} \quad (31)$$

For the SIS lens model, from Eq. (14), the amplification factor is written analytically (see Appendix A for derivation),

$$F(w, y) = e^{\frac{i}{2}wy^2} \sum_{n=0}^{\infty} \frac{\Gamma(1 + \frac{n}{2})}{n!} (2we^{i3\pi/2})^{n/2} {}_1F_1\left(1 + \frac{n}{2}, 1; -\frac{i}{2}wy^2\right). \quad (32)$$

Hence, the magnification is written as

$$\mu(w, y) = \left| \sum_{n=0}^{\infty} \frac{\Gamma(1 + \frac{n}{2})}{n!} (2we^{i3\pi/2})^{n/2} {}_1F_1\left(-\frac{n}{2}, 1; \frac{i}{2}wy^2\right) \right|^2. \quad (33)$$

The maximum magnification is given by setting  $y = 0$ ,

$$\mu_{max} = \left| \sum_{n=0}^{\infty} \frac{\Gamma(1 + \frac{n}{2})}{n!} (2we^{i3\pi/2})^{n/2} \right|^2 \quad (34)$$

$$= \left| 1 + \frac{1}{2}(1 - i)e^{-\frac{i}{2}w} \sqrt{\pi w} \left[ 1 + \text{Erf}\left(\frac{\sqrt{w}}{2}(1 - i)\right) \right] \right|^2, \quad (35)$$

where  $\text{Erf}(z)$  is the error function (see Appendix A).

Figure 4 shows the magnification  $\mu(w, y)$  for the SIS model as a function of  $w$  with the dimensionless source position fixed as  $y = 0.1, 0.5, \text{ and } 1$ , respectively. Note that when  $y = 1$  (a single image is formed in the geometrical optics limit), the oscillatory behavior appears. Our result is consistent with the previous result [30, 31].

Finally in this section let us consider the amplification factor based on the geometrical optics estimation. In the SIS lens model, the two stationary points (the minimum and the saddle points) appear for  $y < 1$ , while only one stationary point appears for  $y \geq 1$ . Therefore we have

$$F_{geo}(w, y) = \begin{cases} |\mu_+|^{1/2} e^{(-iw(y+1/2))} - i|\mu_-|^{1/2} e^{(iw(y+1/2))} & (y < 1), \\ |\mu_+|^{1/2} & (y \geq 1), \end{cases} \quad (36)$$

from Eq. (18), where  $\mu_{\pm} = \pm 1 + 1/y$ . Then, the magnification in the geometrical optics is written

$$\mu_{geo}(w, y) = \begin{cases} 2/y + 2\sqrt{-1 + 1/y^2} \sin(2wy) & (y < 1), \\ 1 + 1/y & (y \geq 1). \end{cases} \quad (37)$$



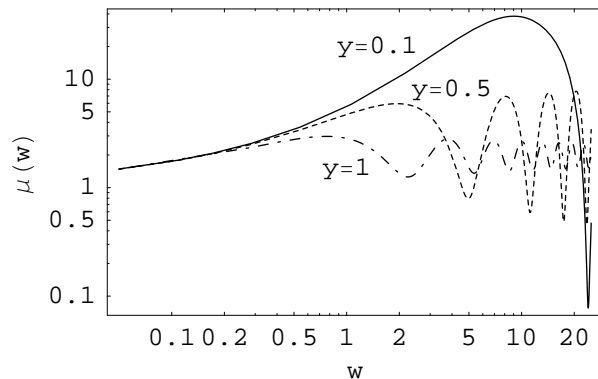


**Figure 4.** Same as figure 2 but for the SIS lens model. The behavior is very similar to that in Figure 2.

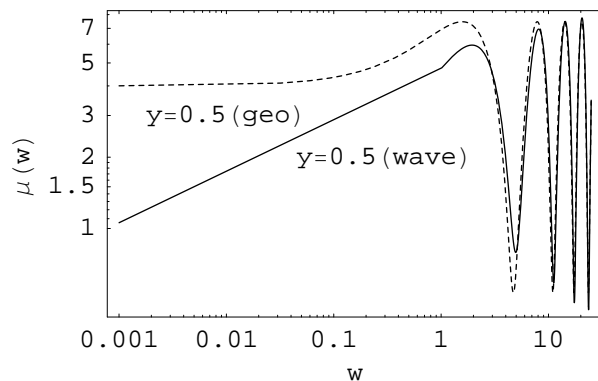


**Figure 5.** Same as figure 3 but for the SIS lens model. The solid curve is the magnification  $\mu(w, y)$  and the dashed curve is the corresponding geometrical optics formula  $\mu_{geo}(w, y)$ . Here, the source position is fixed as  $y = 0.5$ . The geometrical optics approximation is not valid for  $w \lesssim 1$ .

Figure 5 compares the magnification (33) and (37) as a function of the parameter  $w$ , where the source position is fixed as  $y = 0.5$ .

#### 4. Magnification of an Extended Source

In this section we investigate the finite source size effect in the wave optics. We consider the magnification from an extended source with a Gaussian distribution of the surface brightness. The analytic formulas for the magnification in the previous section are useful in the investigation in this section.

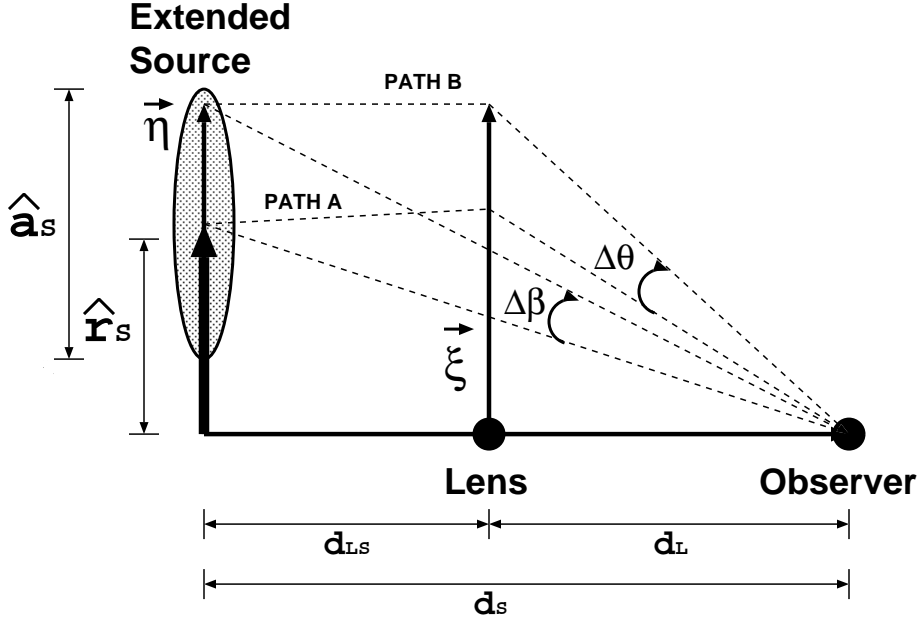


**Figure 6.** Configuration of the gravitational lens system for an extended source. Here,  $d_L$ ,  $d_S$  and  $d_{LS}$  are the angular diameter distances between the observer and the lens, between the observer and the source, between the lens and the sources, respectively.  $\xi$  and  $\eta$  are the dimensional coordinates in the lens and the source planes, respectively.  $\hat{r}_S$  specifies the position of the source center, and  $\hat{a}_S$  is the source size. This sketch is based on the thin lens approximation.

#### 4.1. Formulation

Following Ref. [32], we consider the integral of the point source magnification weighted by the source intensity

$$\bar{\mu}(w, a_S, r_S) = \frac{\int_{-\infty}^{\infty} W(\vec{y}) \mu(w, y) d^2y}{\int_{-\infty}^{\infty} W(\vec{y}) d^2y}, \quad (38)$$

where we assume the Gaussian distribution of the source intensity

$$W(\vec{y}) = \exp\left(-\frac{|\vec{y} - \vec{Y}|^2}{2a_S^2}\right), \quad (39)$$

where  $\vec{Y}$  ( $|\vec{Y}| = r_S$ ) specifies the dimensionless source position, and  $a_S$  is the dimensionless source size. These dimensionless quantities of the source position and the source size are related to the dimensional quantities by

$$r_S = \frac{\hat{r}_S}{d_S \theta_E}, \quad a_S = \frac{\hat{a}_S}{d_S \theta_E}, \quad (40)$$

where  $\hat{r}_S$  and  $\hat{a}_S$  are the source position and the source size, respectively (see Figure 6). Note that the modified magnification depends on the source size  $a_S$  as well as the source position  $r_S$ .

We find the magnification can be written as

$$\bar{\mu}(w, a_S, r_S) = \frac{1}{a_S^2} e^{-\frac{r_S^2}{2a_S^2}} \int_0^{\infty} dy y e^{-\frac{y^2}{2a_S^2}} I_0\left(\frac{r_S}{a_S} y\right) \mu(w, y), \quad (41)$$

where  $I_0(z)$  is the modified Bessel function of the zeroth order.

We will find the analytic expression for the integral (41) with the use of the result obtained in the previous section. Using the Taylor expansion of the magnification  $\mu(w, y)$  around  $y = r_S$ ,

$$\mu(w, y) = \sum_{n=0}^{\infty} \frac{1}{n!} \mu^{(n)}(w, y = r_S) (y - r_S)^n, \quad (42)$$

where  $\mu^{(n)}(w, y)$  is the n-rank derivative of  $\mu(w, y)$  with respect to  $y$ , the magnification (41) can be written in the form

$$\bar{\mu}(w, a_S, r_S) = \sum_{n=0}^{\infty} A_n \mu^{(n)}(w, y = r_S), \quad (43)$$

where the coefficient is

$$A_n = \frac{1}{a_S^2 n!} e^{-\frac{r_S^2}{2a_S^2}} \int_0^{\infty} dy y e^{-\frac{y^2}{2a_S^2}} I_0\left(\frac{r_S}{a_S} y\right) (y - r_S)^n. \quad (44)$$

We can evaluate the coefficients in an analytic manner. For example, for the first two terms, we have

$$A_0 = 1, \quad (45)$$

$$A_1 = a_S \left[ -\frac{r_S}{a_S} + \sqrt{\frac{\pi}{2}} e^{-\frac{r_S^2}{4a_S^2}} \left( \left( 1 + \frac{r_S^2}{2a_S^2} \right) I_0\left(\frac{r_S}{2a_S}\right) + \frac{r_S^2}{2a_S^2} I_1\left(\frac{r_S}{2a_S}\right) \right) \right] \quad (46)$$

$$\simeq \begin{cases} a_S^2/r_S & (r_S \gg a_S) \\ a_S \sqrt{\pi/2} & (r_S \ll a_S) \end{cases}, \quad (47)$$

where  $I_1(z)$  is the modified Bessel function of the first order. The other terms can be evaluated in a similar way. Note that the zeroth order term of Eq. (43) reproduces the magnification of the point source. Hence, our expression (43) is based on the expansion around the point source limit.

#### 4.2. Point Mass Lens

For the point mass lens case, with the use of the expression (24), we can evaluate the magnification of the extended source. Here, we write the first two terms,

$$\bar{\mu}(w, a_S, r_S) \simeq A_0 \mu^{(0)}(w, r_S) + A_1 \mu^{(1)}(w, r_S) \quad (48)$$

$$= \mu(w, r_S) \left[ 1 - A_1 w^2 r_S \Re \left[ \frac{{}_1F_1(1 + \frac{i}{2}w, 2; \frac{i}{2}wr_S^2)}{{}_1F_1(\frac{i}{2}w, 1; \frac{i}{2}wr_S^2)} \right] \right]. \quad (49)$$

For the point mass lens model, with the use of the approximate expression (27), the magnification of the extended source is evaluated in the geometrical optics. Figure 7 shows  $\bar{\mu}(w, a_S, r_S)$  and the corresponding magnification with the geometrical optics approximation. Here, in evaluating  $\bar{\mu}(w, a_S, r_S)$ , we summed the terms up to  $n = 20$ , and the position of the source center and the radius of the source are fixed as  $a_S = 0.5$  and  $r_S = 0.5$ , respectively. Note that both the curves agree for  $w \gtrsim 1$ . Comparing it with Figure 3, the oscillation-amplitude decreases as  $w$  becomes large.

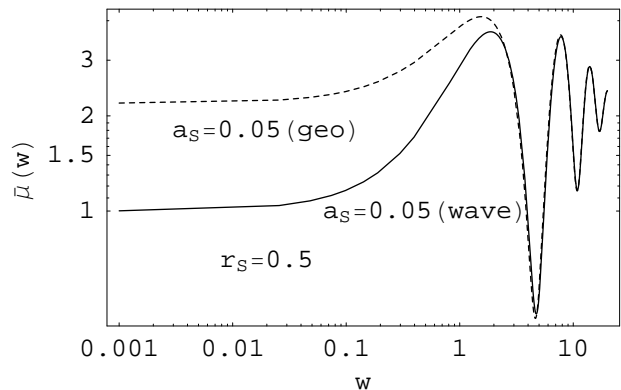


**Figure 7.** The magnification of the extended source  $\bar{\mu}(w, a_S, r_S)$  for the point mass lens model, as a function  $w$ . Here, the position of the source center and the source radius are fixed  $r_S = 0.5$  and  $a_S = 0.5$ . For  $w \gtrsim 1$ , the wave optics agrees with the geometrical optics.

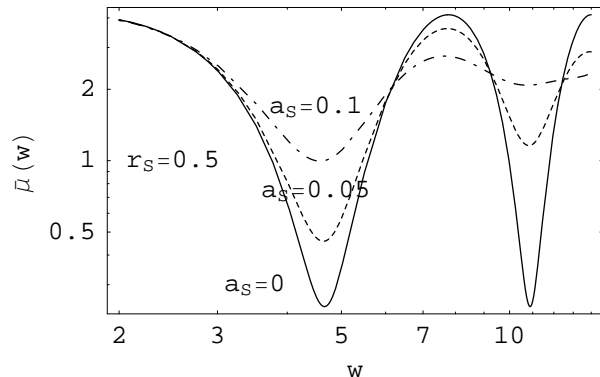


**Figure 8.** The magnification  $\bar{\mu}(w, a_S, r_S)$  as a function of  $w$  for the point mass lens model. Here, the position of the source center is fixed as  $r_S = 0.5$ , and the three curves show the different source sizes specified by  $a_S = 0$ ,  $a_S = 0.05$  and  $a_S = 0.1$ , respectively. As the source size becomes larger, the oscillation-amplitude of the magnification decreases. In the computation of this magnification, we used the approximation of the geometrical optics. This provides a good approximation as long as  $w \gtrsim 1$ , as demonstrated in figure 7.

Figure 8 plots the magnification of the extended source, as a function of  $w$ . Here, the source position is fixed as  $r_S = 0.5$ , and the three curves assume the source size  $a_S = 0$ ,  $a_S = 0.05$ , and  $a_S = 0.1$ , respectively. As the source size becomes larger, the oscillation-amplitude of the magnification decreases. This can be understood as follows. The oscillation feature comes from the interference of two waves in the geometrical optics in the case of the point source. In the case of an extended source, the wave magnification is determined by a superposition of many waves. Then, the clear interference disappears by averaging over the phase.

Now let us evaluate the condition that the finite source size effect becomes substantial in an analytic manner. The ratio of the second term to the first term

of the right hand side of Eq. (49) is

$$\delta\bar{\mu}/\mu = -A_1 w^2 r_S \Re \left[ \frac{{}_1F_1(1 + \frac{i}{2}w, 2; \frac{i}{2}wr_S^2)}{{}_1F_1(\frac{i}{2}w, 1; \frac{i}{2}wr_S^2)} \right] \quad (50)$$

$$\simeq -w^2 r_S A_1 + \mathcal{O}(w^4). \quad (51)$$

The condition that the finite source size effect becomes substantial is  $|\delta\bar{\mu}/\mu| \sim \mathcal{O}(1)$ . For the case  $r_S \gg a_S$ , we may approximate  $A_1 \simeq a_S^2/r_S$ , and we have

$$\delta\bar{\mu}/\mu \simeq -(a_S w)^2. \quad (52)$$

Thus,  $a_S w$  is a key parameter of the finite source size effect in the wave optics.

Next, let us examine the finite source size effect near the caustic  $r_S = 0$  in detail. Some aspects have been discussed in Ref. [15]. The above argument is based on the expansion of the magnification in terms of  $w$ , which is not suitable for the large value of  $w$ . We here consider the regime of the geometrical optics. In the limit  $w \gg 1$  and  $y \ll 1/w^{1/2}$ , we may write

$$\mu(w, y) = \pi w J_0(wy)^2, \quad (53)$$

where we used the mathematical formula [35]

$$\lim_{a \rightarrow \infty} {}_1F_1(a, 1; z/a) = I_0(2\sqrt{z}) \quad (54)$$

with  $z$  fixed. Note that the approximate formula (53) is rather general, which can be derived from (14) with the saddle point method for  $w \gg 1$  ([15], see also below).

Substituting (53) into (41), the magnification can be evaluated as

$$\bar{\mu}(w, a_S, r_S) = \frac{\pi w}{a_S^2} e^{-\frac{r_S^2}{2a_S^2}} \int_0^\infty dy y e^{-\frac{y^2}{2a_S^2}} I_0\left(\frac{r_S}{a_S} y\right) J_0(wy)^2, \quad (55)$$

which is valid for  $r_S < a_S \ll 1/w^{1/2} \ll 1$ . Using the definition of the modified Bessel function

$$I_0(z) = \sum_{m=0}^{\infty} \frac{z^{2m}}{(m!)^2 2^{2m}}, \quad (56)$$

we can write

$$\bar{\mu}(w, a_S, r_S) = \frac{\pi w}{a_S^2} e^{-\frac{r_S^2}{2a_S^2}} \sum_{m=0}^{\infty} (-1)^m \frac{(r_S/a_S^2)^{2m}}{(m!)^2 2^{2m}} \frac{\partial^m \alpha_0(\beta)}{\partial \beta^m} \Big|_{\beta=1/2a_S^2}, \quad (57)$$

where we defined

$$\alpha_0(\beta) = \int_0^\infty dy y e^{-\beta y^2} J_0(wy)^2 = \frac{1}{2\beta} e^{-w^2/2\beta} I_0(w^2/2\beta). \quad (58)$$

Using the condition,  $r_S < a_S \ll 1/w^{1/2} \ll 1$ , the first two terms of (57) yield

$$\bar{\mu}(w, a_S, r_S) \simeq \pi w e^{-r_S^2/2a_S^2} e^{-w^2 a_S^2} I_0(w^2 a_S^2) \left( 1 + \frac{1}{2} \frac{r_S^2}{a_S^2} \right), \quad (59)$$

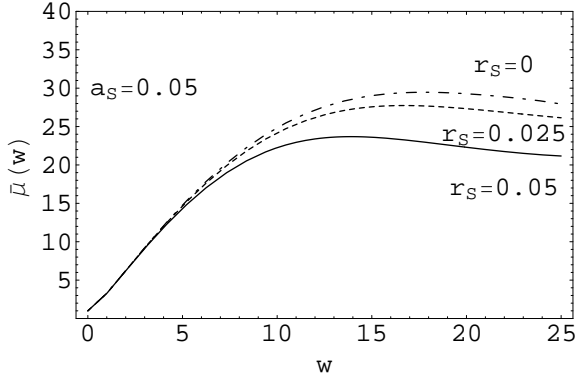


**Figure 9.** Magnification  $\bar{\mu}(w, a_S, r_S)$  as a function of  $w$ . Here, the source size is fixed as  $a_S = 0.05$ , and the position of the source center is  $r_S = 0, 0.025$ , and  $0.05$ , respectively.

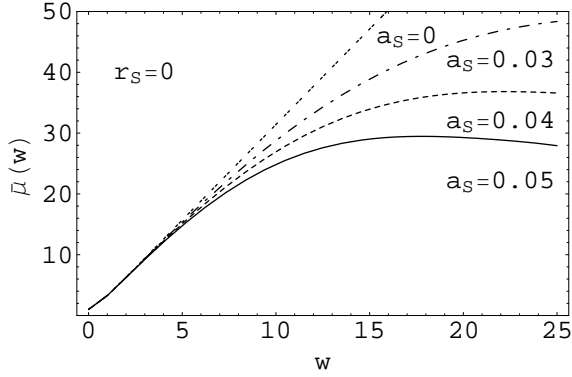


**Figure 10.** Magnification  $\bar{\mu}(w, a_S, r_S)$  as a function of  $w$ . Here, the position of the source center is fixed as  $r_S = 0$ , and the source size is  $a_S = 0, 0.03, 0.04$ , and  $0.05$ , respectively.

which reduces to

$$\bar{\mu}(w, a_S, r_S) \simeq \begin{cases} \pi w e^{-r_S^2/2a_S^2} \left(1 + \frac{1}{2} \frac{r_S^2}{a_S^2}\right) \\ \quad = \pi w \left(1 + \mathcal{O}(r_S^4/a_S^4)\right) & (wa_S \ll 1) \\ \sqrt{\frac{\pi}{2}} \frac{1}{a_S} e^{-r_S^2/2a_S^2} \left(1 + \frac{1}{2} \frac{r_S^2}{a_S^2}\right) \\ \quad = \sqrt{\frac{\pi}{2}} \frac{1}{a_S} \left(1 + \mathcal{O}(r_S^4/a_S^4)\right) & (wa_S \gg 1) \end{cases}. \quad (60)$$

This expression means the followings: the result of the point source is reproduced for  $wa_S \ll 1$  and  $r_S = 0$ , while the finite source size effect becomes substantial for  $wa_S \gg 1$  and  $\bar{\mu}$  approaches to the constant value  $\sqrt{\pi/2}/a_S$  for  $r_S = 0$ . The magnification  $\bar{\mu}$  becomes smaller as  $r_S/a_S$  becomes large.

Figure 9 shows  $\bar{\mu}(w, a_S, r_S)$  as a function of  $w$  with the source size  $a_S = 0.05$  for the different source position  $r_S = 0, 0.025$ , and  $0.05$ , respectively. In this figure we see

that  $\bar{\mu}$  approaches a constant value ( $\sim 1/a_S$ ) slightly depending on  $r_S$ , as  $w$  becomes large. Figure 10 plots  $\bar{\mu}(w, a_S, r_S)$  with the source position fixed as  $r_S = 0$ , and the different source size  $a_S = 0, 0.03, 0.04, \text{ and } 0.05$ , respectively. Even for the Einstein ring configuration, due to the finite source size effect, the maximum amplification is limited by the factor ( $\sim 1/a_S$ ) for  $w \gtrsim 1/a_S$ . These behaviors are consistent with those expected from the above analytic argument.

The above results demonstrate that the condition that the finite source size effect becomes substantial is  $wa_S > 1$ . The reason can be understood as follows: As shown in Appendix B, the condition,  $wa_S = 1$ , is equivalent to the condition that the path difference between the PATH A and the PATH B in Figure 6 becomes comparable to the wavelength. Therefore, the observed wave is a superposition of many waves with different phases for  $wa_S \gg 1$ . This eliminates the interference feature and decreases the oscillation feature in the energy spectrum. The finite source size effect near the caustic  $r_S = 0$  is also understood in the similar way. The maximum magnification is decreased by averaging over the magnification of different phases that depend on the position on the source surface.

#### 4.3. Singular Isothermal Sphere Lens

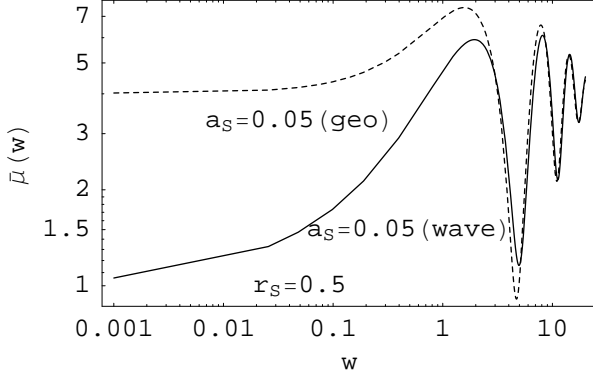
We here consider the finite source size effect in the SIS lens model. In this case, the magnification of the extended source (43) can be evaluated with the expression (33). Figure 11 shows the magnification  $\bar{\mu}$  (solid curve), where we set  $r_S = 0.5$  and  $a_S = 0.5$ . The dashed curve is the corresponding geometrical optics with (37) instead of (33). In the numerical computation, we performed the sum with respect to  $n$  up to 20.

Figure 12 plots the magnification of the extended source, as a function of  $w$ . Here, the source position is fixed as  $r_S = 0.5$ , and the three curves assume the source size  $a_S = 0, a_S = 0.05, \text{ and } a_S = 0.1$ , respectively. As the source size becomes larger, the oscillation-amplitude of the magnification decreases. Similarly to the case of the point mass lens model, the clear oscillation feature disappears as the source size becomes large. In this figure we used the approximation of the geometrical optics in evaluating the magnification because of a convenience of numerical technique. The validity of its approximation is demonstrated in Figure 11 at least for  $w \gtrsim 5$ . The approximation is not very good for  $w \lesssim 5$ , however, it does not alter our conclusions.

We write down the first two terms of the magnification

$$\bar{\mu}(w, r_S, a_S) \simeq A_0 \mu^{(0)}(w, r_S) + A_1 \mu^{(1)}(w, r_S), \quad (61)$$

$$\begin{aligned} &= \mu(w, r_S) \left[ 1 - A_1 w r_S \right. \\ &\quad \times \Re \left[ \frac{\sum_{n=0}^{\infty} \frac{\Gamma(1+\frac{n}{2})}{n!} (-in) (2we^{i3\pi/2})^{n/2} {}_1F_1(1 - \frac{n}{2}, 2; \frac{i}{2} w r_S^2)}{\sum_{n=0}^{\infty} \frac{\Gamma(1+\frac{n}{2})}{n!} (2we^{i3\pi/2})^{n/2} {}_1F_1(-\frac{n}{2}, 1; \frac{i}{2} w r_S^2)} \right] \Big]. \end{aligned} \quad (62)$$



**Figure 11.** Same as Figure 7, but for the SIS lens model. For  $w \gtrsim 5$ , the difference between the wave optics and the geometrical optics is negligible. Here, we fixed  $r_S = 0.5$  and  $a_S = 0.5$ .

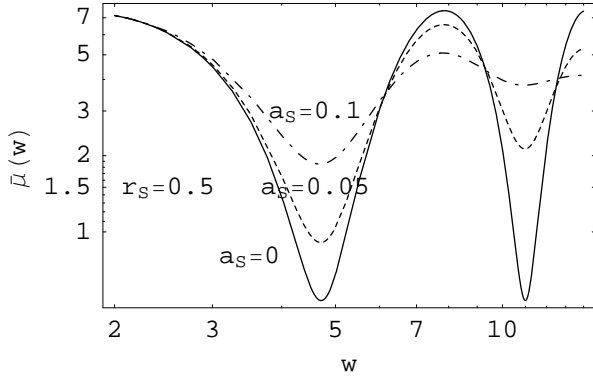


**Figure 12.** Same as Figure 8, but for the SIS lens model. Here, the position of the source center is fixed  $r_S = 0.5$ , and the magnification is plotted for  $a_S = 0, 0.05$ , and  $0.1$ , respectively.

The ratio of the second term to the first term of the right hand side of Eq. (62) is

$$\delta\bar{\mu}/\mu = -A_1 w r_S \times \Re \left[ \frac{\sum_{n=0}^{\infty} \frac{\Gamma(1+\frac{n}{2})}{n!} (-in) (2we^{i3\pi/2})^{n/2} {}_1F_1(1-\frac{n}{2}, 2; \frac{i}{2}wr_S^2)}{\sum_{n=0}^{\infty} \frac{\Gamma(1+\frac{n}{2})}{n!} (2we^{i3\pi/2})^{n/2} {}_1F_1(-\frac{n}{2}, 1; \frac{i}{2}wr_S^2)} \right] \quad (63)$$

$$\simeq -\frac{\sqrt{\pi}}{2} w^{3/2} r_S A_1 + \left(2 - \frac{\pi}{2}\right) w^2 r_S A_1 + \mathcal{O}(w^{5/2}). \quad (64)$$

The condition that the point source approximation breaks is  $|\delta\bar{\mu}/\mu| \sim \mathcal{O}(1)$ . In the limit  $r_S \gg a_S$ , we have  $A_1 \simeq a_S^2/r_S$ , then

$$\delta\bar{\mu}/\mu \simeq -\frac{\sqrt{\pi}}{2} a_S^2 w^{3/2} + \left(2 - \frac{\pi}{2}\right) w^2 a_S^2 + \mathcal{O}(w^{5/2}). \quad (65)$$

Next, similarly to the point mass lens model, we examine the finite source size effect near the caustic  $r_S = 0$ . Here, let us consider the approximate estimation of Eq. (14) using the saddle point method, as demonstrated in Ref. [15]. Using the approximate



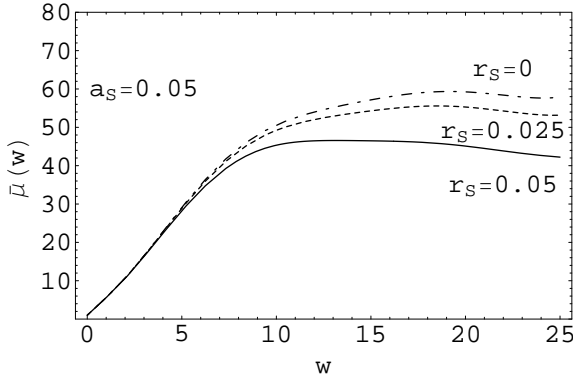


**Figure 13.** Same as Figure 9, but for the SIS lens model.

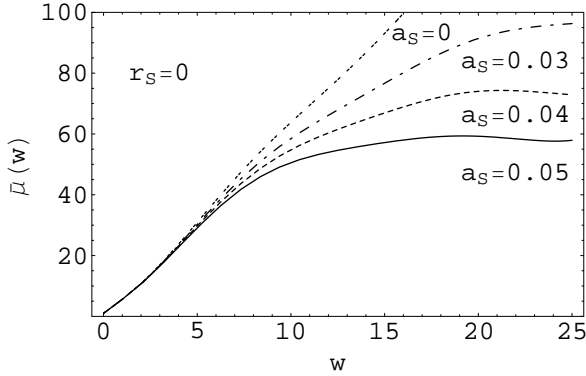


**Figure 14.** Same as Figure 10, but for the SIS lens model.

method, for  $w \gg 1$  and  $y \ll 1/\sqrt{w}$ , we obtain

$$\mu(w, y) \simeq \frac{2\pi w x_*^2}{|1 - \psi''(x_*)|} J_0(w x_* y)^2, \quad (66)$$

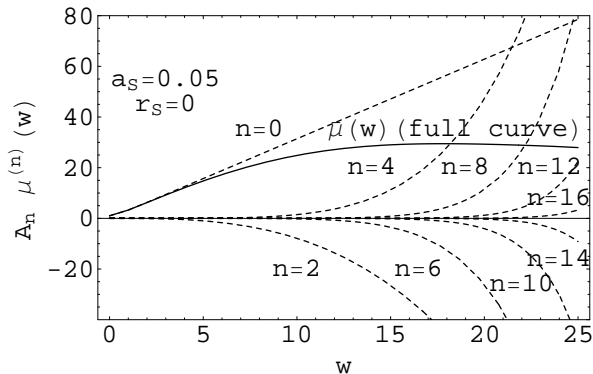
where  $x_*$  is a positive solution of the lens equation  $x = \psi'(x)$ . For the SIS model, we have

$$\mu(w, y) \simeq 2\pi w J_0(wy)^2. \quad (67)$$

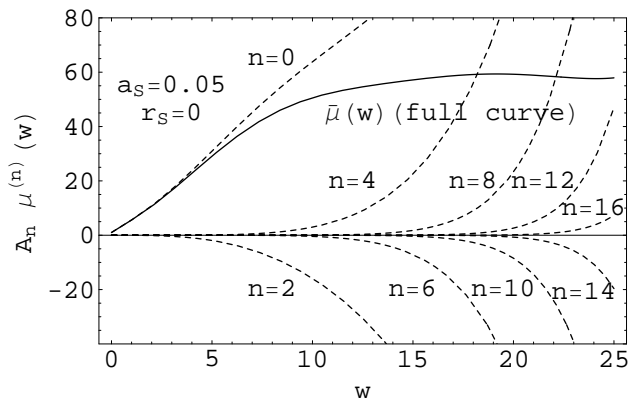
Substituting Eq. (67) into (41), we have the same expressions of the magnification as Eqs. (55) and (60), but with multiplied by the constant factor 2.

Figure 13 shows  $\bar{\mu}(w, a_S, r_S)$  as a function of  $w$  with the source size  $a_S = 0.05$  for the different source position  $r_S = 0, 0.025$ , and  $0.05$ , respectively, for the SIS lens model. Similarly, Figure 14 plots  $\bar{\mu}(w, a_S, r_S)$  with the source position fixed as  $r_S = 0$ , and the different source size  $a_S = 0, 0.03, 0.04$ , and  $0.05$ , respectively. These figures show the similar behaviors to those in the point mass lens model.

Finally in this section, we mention our computation and the numerical convergence. We have performed the numerical computation using the package MATHEMATICA. The terms in Eq. (43) with respect to  $n$  are summed up to  $n = 20$ . The dashed curves in Figure 15 shows each term of  $A_n \mu^{(n)}$  as a function  $w$  for the point mass lens model,



**Figure 15.**  $A_n \mu^{(n)}$  in Eq. (43) as a function of  $w$  for the point mass lens model. The dashed curves are the terms for  $n = 0, 2, 4, 6, 8, 12, 14,$  and  $16$ , respectively, while the solid curve is the sum up to the term for  $n = 20$ . Here, we fixed the parameters as  $a_S = 0.05$  and  $r_S = 0$ .



**Figure 16.** Same as Figure 15, but for the SIS lens model.

where we adopted the parameters  $a_S = 0.05$  and  $r_S = 0$ . The solid curve is the (summed) magnification  $\bar{\mu}(w)$ . Figure 16 is same as Figure 15 but for the SIS lens model. As long as  $w \lesssim 20$ , the convergence of our computation is evident. But for the large value of  $w$ , our method is not advantageous because higher terms with respect to  $n$  is required. The numerical methods developed in Refs. [15, 30, 31] would be useful for numerical computation of general cases.

## 5. Discussion

In this section, let us discuss astrophysical consequences of the result in the previous section. We first summarize the conditions that the lensing signature of the wave optics may appear in the spectral feature, as follows:

$$w \sim 1, \tag{68}$$

$$|\delta \bar{\mu} / \bar{\mu}| \lesssim 1. \tag{69}$$

The first condition (68) is that the wave optics in lensing becomes important for a monochromatic wave from a point source. The second condition (69) is that the oscillation feature in energy spectra survives against the finite source size effect. Here, we consider the case  $r_S \gtrsim a_S$ . Therefore, with Eqs. (52) and (65), combination of both the condition simply gives  $a_S \lesssim 1$ .

Then, we discuss possible observational consequences of the wave effect in the astrophysical situation, the lensing of the gravitational wave from a binary compact objects [15] and the *femtolensing* of the gamma ray burst [32, 33].

### 5.1. Gravitational Wave from a Compact Binary

For the point mass lens model, the dimensionless parameter  $w$  is given by Eq. (23). The condition  $w \sim 1$  yields

$$\left(\frac{\nu}{1\text{Hz}}\right) \sim \frac{0.8}{1+z_L} \left(\frac{M}{10^4 M_\odot}\right)^{-1}. \quad (70)$$

We also have

$$a_S \simeq 1 \times 10^{-11} \left(\frac{\hat{a}_S}{10^3 \text{km}}\right) \left(\frac{M}{10^4 M_\odot}\right)^{-1/2} \left(\frac{H_0^{-1}}{d_{LS} d_S / d_L}\right)^{1/2}, \quad (71)$$

where  $H_0^{-1} = (70 \text{km/s/Mpc})^{-1} = 1.3 \times 10^{26} \text{m}$  is the Hubble distance. On the other hand, for the SIS model,  $w$  is given by (31). Then, from  $w \sim 1$ , we have

$$\left(\frac{\nu}{1\text{Hz}}\right) \sim \frac{20}{1+z_L} \left(\frac{\sigma_v}{1\text{km/s}}\right)^{-4} \left(\frac{d_L d_{LS} / d_S}{H_0^{-1}}\right)^{-1}. \quad (72)$$

We also have

$$a_S \simeq 6 \times 10^{-11} \left(\frac{\hat{a}_S}{10^3 \text{km}}\right) \left(\frac{\sigma_v}{1\text{km/s}}\right)^{-2} \left(\frac{H_0^{-1}}{d_{LS}}\right). \quad (73)$$

Let us consider the binary compact objects, which consists of the two equal objects with the mass  $m$ . For the binary we have the relation  $(Gm)^2/2L = 4^{-2/3}(Gm)^{5/3}(\omega/2)^{2/3}$ , where  $L$  is the distance between the two objects and  $\omega$  is the angular frequency of the gravitational wave. This equation is rewritten as

$$L \simeq 3 \times 10^3 \left(\frac{m}{M_\odot}\right)^{1/3} \left(\frac{\nu}{1\text{Hz}}\right)^{-2/3} \text{km}. \quad (74)$$

If we set  $L \sim \hat{a}_S$ , it is clear that  $a_S \ll 1$  as long as we consider the gravitational wave of the frequency around 1Hz. This means that the point source approximation is very good for the gravitational wave of this frequency.

### 5.2. Femtolensing

We next consider the femtolensing, which was pointed out by Gould, and Stanek, Paczynski and Goodman [32, 33]. The femtolensing is the lens effect by a tiny mass on the gamma ray burst.

For the point mass lens model, the condition  $w \sim 1$  is rewritten as

$$\left(\frac{h\nu}{1\text{keV}}\right) \sim \frac{0.7}{1+z_L} \left(\frac{M}{10^{20}\text{g}}\right)^{-1}, \quad (75)$$

where  $h$  is the Planck constant. The dimensionless source size may be written as

$$a_S \simeq 0.5 \times \left(\frac{\hat{a}_S}{10^5\text{km}}\right) \left(\frac{M}{10^{20}\text{g}}\right)^{-1/2} \left(\frac{H_0^{-1}}{d_{LS}d_S/d_L}\right)^{1/2}. \quad (76)$$

This suggests that the finite source size effect is important in the femtolensing by the point mass lens. If the source size is larger than  $10^5\text{km}$ , the finite source size effect becomes significant. In this case the signature of the interference in energy spectra will disappear.

On the other hand, for the SIS model, (72) is rewritten as

$$\left(\frac{h\nu}{1\text{keV}}\right) \sim \frac{0.8}{1+z_L} \left(\frac{\sigma_v}{0.1\text{m/s}}\right)^{-4} \left(\frac{d_L d_{LS}/d_S}{H_0^{-1}}\right)^{-1}. \quad (77)$$

We also have

$$a_S \simeq 0.5 \times \left(\frac{\hat{a}_S}{10^5\text{km}}\right) \left(\frac{\sigma_v}{0.1\text{m/s}}\right)^{-2} \left(\frac{H_0^{-1}}{d_{LS}}\right). \quad (78)$$

This suggests that the femtolensing might have occurred due to a very small mass halo, if it existed. Such the very small mass halo might be unrealistic in our universe, (cf. [37]). However, Moore et al. have pointed out the possibility of the survival of very small mass halos which are produced in the high redshift universe, depending on the dark matter model [38], though the possibility is still open to debate [40, 39, 41]. Our investigation suggests that the source size is a crucial factor even if the femtolensing occurred by such the very small halo. When the source size is larger than  $10^5\text{km}$ , the interference signature will be significantly affected by the finite source size effect.

### 5.3. Finite Source Size Effect near the Caustic

We now consider the finite source size effect in the wave optics near the caustic. We have demonstrated that it becomes influential when  $a_S w \gtrsim 1$  for  $a_S \ll 1/\sqrt{w} \ll 1$ . For the gravitational wave from a compact binary,  $a_S w \ll 1$  will be reasonable for general situation. Hence, we here consider the femtolensing. We may write

$$a_S w \simeq 0.7 \times (1+z_L) \left(\frac{h\nu}{1\text{keV}}\right) \left(\frac{M}{10^{20}\text{g}}\right)^{1/2} \left(\frac{\hat{a}_S}{10^5\text{km}}\right) \left(\frac{H_0^{-1}}{d_{LS}d_S/d_L}\right)^{1/2}, \quad (79)$$

for the point mass lens mode,

$$a_S w \simeq 0.7 \times (1+z_L) \left(\frac{h\nu}{1\text{keV}}\right) \left(\frac{\sigma_v}{0.1\text{m/s}}\right)^2 \left(\frac{\hat{a}_S}{10^5\text{km}}\right) \left(\frac{d_L}{d_S}\right), \quad (80)$$

for the SIS lens model, respectively. These estimations suggest that the finite source size effect is important in the femtolensing near the caustic too.

## 6. Summary and Conclusions

In this paper we investigated the finite source size effect on the wave optics in the gravitational lensing. First we presented the analytic expression of the magnification for the SIS lens model as well as the point mass lens model. Based on the result, we evaluated the magnification of the finite-size source, assuming a Gaussian profile for the surface intensity. The analytic expression of the magnification is given in terms of the expansion with respect to the source size. This expression is useful to understand how the finite source size effect works on the spectral feature of the magnification in the wave optics. The condition that the finite source size effect becomes significant is discussed. As application of the result, we considered the finite source size effect on the wave optics in lensing of the gravitational wave from a compact binary and the femtolensing. For the lensing of the gravitational wave, it is demonstrated that the finite source size effect can be negligible as long as we consider the gravitational wave of the frequency around 1Hz. For the femtolensing of the gamma ray burst, we confirmed the result by Stanek et al. [32], for the point mass lens model. We also considered the femtolensing by the hypothetically very small halo. The femtolensing might imprint the lensing signature on energy spectra if occurred, however, the finite source size effect is crucial. If the source size is larger than  $10^5\text{km}$ , the finite source size effect becomes significant and will not allow the detection of the interference signature in the energy spectra.

It is worthy noting the finite source size effect near the caustic. In the wave optics of the lens configuration of the Einstein ring, the maximum magnification of the point source is not divergent, but is in proportion to the frequency of the wave. But, for an extended sources, the finite source size effect becomes substantial for  $a_S w \gtrsim 1$ , in which the maximum magnification is suppressed by the value  $\sqrt{\pi/2}/a_S$  as long as  $a_S \ll 1/\sqrt{w} \ll 1$ . This finite source size effect would be influential in the femtolensing near the caustic too, if the source size is larger than  $10^5\text{km}$ .

## Acknowledgments

All the numerical computation presented in this paper were performed with the help of the package MATHEMATICA version 5.0. The authors thank an anonymous referee for useful comments which helped improve the manuscript. We are also grateful to Y. Kojima, R. Yamazaki, M. Sakagami, K. Nakao, C. Yoo and R. Takahashi for useful comments and conversations related to the topic in the present paper.

## References

- [1] Schneider P, Ehlers J and Falco E E 1992 *Gravitational Lenses* (Springer-Verlag: Berlin)
- [2] *Gravitational Lensing and the High-Redshift Universe*, 1999 Prog. of Theor. Phys. Suppl. No. 133 ed. by Futamase T and Tomita K
- [3] Alcock et al. 1996 *Astrophys. J.* 461 84
- [4] Bacon D, Refregier A, Ellis R 2000 *Mon. Not. R. Astron. Soc.* 318 625

- [5] Wittman D M, Tyson A J, Kirkman D, Dell'Antonio I, and Bernstein G 2000 Nature 405 143
- [6] Kaiser N, Wilson G and Luppino G 2000 astro-ph/0003338
- [7] Maoli R, Van Waerbeke L, Mellier Y, Schneider P, Jain B, Bernardeau F, Erben T and Ford B 2001 A&A 368 766
- [8] Yamamoto K and Futamase T 2001 Prog. Theor. Phys. 105 707
- [9] Yamamoto K, Kadoya Y, Murata T and Futamase T 2001 Prog. Theor. Phys. 106 917
- [10] Tyson J A, Wittman D M, Hennawi J F and Spergel D N, 2002 astro-ph/0209632
- [11] Meneghetti M, Jain N, Bartelmann M and Dolag K 2005 Mon. Not. R. Astron. Soc. 362 1301
- [12] Peters P C 1974 Phys Rev D 9 2207
- [13] Deguchi S and Watson W D 1986 Phys Rev D 34 1708
- [14] Deguchi S and Watson W D 1986 ApJ 307 30
- [15] Nakamura T T and Deguchi S 1999, Prog. Theo. Phys. Suppl. 133 137
- [16] Nakamura T T 1998, Phys. Rev. Lett. 80 1138
- [17] Baraldo C Hosoya A and Nakamura T T 1999 Phys Rev D 59 083001
- [18] de Paolis F, Ingrassi G, Nucita A A and Qadir A 2002 A&A 394 749
- [19] Ruffa A A 1999, Astrophys. J 517 L31
- [20] Takahashi R and Nakamura T 2003 Astrophys. J 596 L231
- [21] Takahashi R 2004 A&A 423 787
- [22] Takahashi R and Nakamura T 2005 Prog. Theor. Phys. 113 63
- [23] Takahashi R, Suyama T and Michikoshi S (astro-ph/0503343)
- [24] Macquart J-P 2004 A&A 422 761
- [25] Yamamoto K 2003 Phys Rev D 68 041302(R)
- [26] Yamamoto K 2003 unpublished (astro-ph/0309696)
- [27] Yamamoto K 2005 Phys Rev D 71 101301(R)
- [28] private communication with Nakao K and Yoo C 2005
- [29] Suyama T, Takahashi R and Michikoshi S 2005 Phys Rev D 72 043001
- [30] Takahashi R 2004 PhD Thesis (unpublished)
- [31] Takahashi R and Nakamura T 2003 Astrophys. J 595 1039
- [32] Stanek K Z, Paczynski B and Goodman J 1993 Astrophys. J 413 L7
- [33] Gould A 1992 Astrophys. J 386 L5
- [34] Abramowitz M and Stegun I A 1970 Handbook of Mathematical Functions (Dover: New York)
- [35] Magnus W, Oberhettinger F and Soni R P 1966 Formulas and Theorems for the Special Functions of Mathematical Physics (Springer Verlag: New York)
- [36] Gradshteyn I S and Ryzhik I M 1965 Table of Integrals, Series, and Products (Academic Press: San Diego)
- [37] Kolb E W and Tkachev I I 1996 Astrophys. J 460 L2
- [38] Diemand J, Moore B, Stadel J 2005 Nature 433 389
- [39] Zhao H-S, Taylor J E, Silk J, Hooper D 2005 Archive: astro-ph/0501625
- [40] Moore A, Diemand J, Stadel J, Quinn T 2005. Archive: astro-ph/0502213
- [41] Zhao H-S, Taylor J E, Silk J, Hooper D 2005 Archive: astro-ph/0508215

## Appendix A. Analytic Expression for the Amplification Factor in the SIS Model

In this appendix, we derive an analytic expression of the amplification factor of the SIS lens model. Since the gravitational deflection potential is  $\psi(x) = x$ , Eq. (14) is written

$$F(w, y) = -iwe^{iwy^2/2} \int_0^\infty dx x J_0(wxy) \exp\left[iw\left(\frac{1}{2}x^2 - x\right)\right] \quad (\text{A.1})$$

$$= -iw e^{iwy^2/2} \sum_{n=0}^{\infty} \frac{(-iw)^n}{n!} \int_0^{\infty} dx x^{1+n} J_0(wxy) e^{iwx^2/2}. \quad (\text{A.2})$$

Using a mathematical formula [34], Eq. (A.2) is integrated as

$$F(w, y) = e^{iwy^2/2} \sum_{n=0}^{\infty} \frac{\Gamma(1 + \frac{n}{2})}{n!} (2we^{i3\pi/2})^{n/2} {}_1F_1\left(1 + \frac{n}{2}, 1; -\frac{i}{2}wy^2\right), \quad (\text{A.3})$$

where  ${}_1F_1(a, c, z)$  is the confluent hypergeometric function [35]. Using the formula

$$e^{-z} {}_1F_1\left(-\frac{n}{2}, 1; z\right) = {}_1F_1\left(1 + \frac{n}{2}, 1; -z\right), \quad (\text{A.4})$$

we have

$$F(w, y) = \sum_{n=0}^{\infty} \frac{\Gamma(1 + \frac{n}{2})}{n!} (2we^{i3\pi/2})^{n/2} {}_1F_1\left(-\frac{n}{2}, 1; \frac{i}{2}wy^2\right). \quad (\text{A.5})$$

In the case  $y = 0$ , the Einstein ring configuration, the amplification factor is

$$F(w, y = 0) = -iw \int_0^{\infty} dx x \exp\left(iw \frac{x^2}{2} - iw x\right) \quad (\text{A.6})$$

$$= w \int_0^{\infty} dt t \exp\left(-\frac{w}{2}t^2 - i^{3/2}wt\right). \quad (\text{A.7})$$

Using a mathematical formula [36], we have the analytic simple form

$$F(w, y = 0) = e^{-iw/4} D_{-2}\left(e^{i3\pi/4} \sqrt{w}\right), \quad (\text{A.8})$$

where  $D_{-2}(z)$  is the parabolic cylinder function. With the use of the error function, defined by

$$\text{Erf}(z) = \frac{2}{\sqrt{\pi}} \int_0^z dt e^{-t^2}, \quad (\text{A.9})$$

we may write

$$D_{-2}(z) = \sqrt{\frac{\pi}{2}} e^{z^2/4} z \left(1 - \text{Erf}\left(\frac{z}{\sqrt{2}}\right)\right) - e^{-z^2/4}, \quad (\text{A.10})$$

and we finally have

$$F(w, y = 0) = 1 + \frac{1}{2}(1 - i)e^{-iw/2} \sqrt{\pi w} \left[1 + \text{Erf}\left(\frac{\sqrt{w}}{2}(1 - i)\right)\right]. \quad (\text{A.11})$$

## Appendix B. Path Difference and the Finite Source Size Effect

Here, we consider the path difference between the PATH A and PATH B in Figure 6, and show that  $wa_S = 1$  is equivalent to the condition that the path difference is comparable to the wavelength. Using the angle of the unlensed source position  $\vec{\beta}$  and the angle of the image position  $\vec{\theta}$ , the Fermat's potential is given

$$\hat{\phi}(\theta, \beta) = \frac{d_L d_S}{2d_{LS}} (\vec{\theta} - \vec{\beta})^2 - \hat{\psi}(\theta). \quad (\text{B.1})$$

In the case  $\vec{\beta} = (\beta, 0)$  and  $\vec{\theta} = (\theta, 0)$ , the path difference can be evaluated by

$$\Delta \hat{\phi}(\theta, \beta) = \frac{d_L d_S}{d_{LS}} (\theta - \beta)(\Delta\theta - \Delta\beta) - \hat{\psi}'(\theta) \Delta\theta, \quad (\text{B.2})$$

where we assume  $\Delta\theta \ll \theta$  and  $\Delta\beta \ll \beta$ , and  $\hat{\psi}'(\theta) = d\hat{\psi}(\theta)/d\theta$ , (see Figure 6 for the definitions of  $\Delta\theta$  and  $\Delta\beta$ ).

The gravitational lens equation is given by

$$\frac{d_L d_S}{d_{LS}}(\theta - \beta) - \hat{\psi}'(\theta) = 0, \quad (\text{B.3})$$

and the Einstein angle is defined by the solution of the equation

$$\frac{d_L d_S}{d_{LS}}\theta_E - \hat{\psi}'(\theta_E) = 0. \quad (\text{B.4})$$

With the use of the above equations, we have

$$\Delta\hat{\phi}(\theta, \beta) = -\hat{\psi}'(\theta)\Delta\beta. \quad (\text{B.5})$$

We adopt the approximation for the phase difference,

$$\Delta\hat{\phi}(\theta, \beta) \simeq -\hat{\psi}'(\theta_E)\Delta\beta \simeq -\frac{d_L d_S}{d_{LS}}\theta_E\Delta\beta. \quad (\text{B.6})$$

Because  $\Delta\beta = \hat{a}_S/d_L$ , the condition  $|(1 + z_L)\Delta\hat{\phi}| = \lambda/2\pi$  yields

$$\omega(1 + z_L)\frac{d_L}{d_{LS}}\hat{a}_S\theta_E (= a_S w) = 1, \quad (\text{B.7})$$

where  $\lambda$  is the wavelength of the propagating wave.